

# INVESTIGATION ON THE POSSIBILITY TO USE FORK DETECTOR FOR PARTIAL DEFECT VERIFICATION OF SPENT LWR FUEL ASSEMBLIES

Final report on Task JNT A 1071 (BEL, FIN, SWE)  
of the Member States' Support Programme  
to IAEA Safeguards

A. Tiitta, J. Saarinen (VTT), M. Tarvainen (STUK),  
K. Axell (SKI), P. Jansson (Uppsala University),  
R. Carchon, J. Gerits (SCK•CEN), Y. Kulikov, Y.G. Lee (IAEA)

In STUK this study was supervised by Matti Tarvainen

The conclusions presented in the STUK report series are those of the authors and do not necessarily represent the official position of STUK

ISBN 951-712-589-5 (print)

ISBN 951-712-590-9 (pdf)

ISSN 0785-9325

Dark Oy, Vantaa/Finland 2002

*TIITTA Antero, SAARINEN Johanna (VTT), TARVAINEN Matti (STUK), AXELL Kåre (SKI), JANSSON Peter (Uppsala University), CARCHON Roland, GERITS Jan (SCK•CEN), KULIKOV Yuri, LEE Young-Gil (IAEA). Investigation on the possibility to use fork detector for partial defect verification of spent LWR fuel assemblies. Final report on Task JNT A 1071 (BEL, FIN, SWE) of the Member States' Support Programme to IAEA Safeguards. STUK-YTO-TR 191. Helsinki 2002. 16 pp + Annexes 11 pp.*

**Keywords:** safeguards, partial defect, verification, NDA, spent fuel, LWR, fork detector

## Abstract

The possibility to use a fork detector for partial defect verification of spent LWR fuel assemblies has been investigated in Task JNT A 1071 "Partial Defect Test on Spent Fuel LWRs". The task was arranged as a joint task between the Finnish, Swedish and Belgian support programmes to IAEA safeguards.

This task studied the prospects of both a conventional fork detector and an enhancement where the gross gamma and neutron signals of a conventional fork are combined with simultaneous gamma spectrometry using a CdZnTe detector.

The fork method was investigated by measuring BWR and VVER-440 spent fuel assemblies and a fresh MOX mock-up assembly. Correction methods were developed to improve the analysis of measurement results. Also model calculations were performed to clarify the effect of the geometrical configuration of the defect.

The investigations have shown that a general partial defect test based on the fork method is not possible without making use of operator's declared data. There exist configurations even with 50% of pins removed, which cannot be detected, either with the conventional fork or with the enhanced fork detector. Using the operator declared data cannot be avoided due to the influence of both the fuel design and the irradiation history to the measured signals. If operator's data are available and considered reliable, the detection limit of a partial defect is at about 20% of pins missing for BWR assemblies with the burnup 18 MWd/kg or higher. For developing a reliable, operator data independent partial defect verification device a totally different approach must be applied.

# Contents

ABSTRACT	3
1 INTRODUCTION	5
2 HYPOTHESIS OF THE FORK METHOD IN PARTIAL DEFECT VERIFICATION	6
3 EARLIER INVESTIGATIONS	7
4 EXPERIMENTS AND MODEL CALCULATIONS	8
4.1 BWR and VVER spent fuel assemblies	8
4.1.1 CdZnTe enhancement	8
4.1.2 Using the operator declared data	8
4.1.3 Error sources	9
4.1.4 Neutron versus burnup correlation	10
4.1.5 Neutron versus gamma correlation	11
4.1.6 Model calculations	12
4.2 Mock-up assemblies	13
4.2.1 BWR mock-up assembly	13
4.2.2 PWR mock-up assembly	14
5 CONCLUSION	15
REFERENCES	16
ANNEX 1 MEASURED DEFECT GEOMETRIES OF THE MOX MOCK-UP ASSEMBLY IN BWR 9×9–1 GEOMETRY	17
ANNEX 2 THE MEASURED DATA, BWR MOCK-UP ASSEMBLY	20
ANNEX 3 MEASURED DEFECT GEOMETRIES, MOX MOCK-UP ASSEMBLY IN PWR 17×17–25 GEOMETRY	21
ANNEX 4 THE MEASURED DATA, PWR MOCK-UP ASSEMBLY	27

# 1 Introduction

According to the IAEA's safeguards criteria a partial defect verification of spent fuel assemblies has to be performed before they become difficult to access, i.e. in a deep repository. A partial defect test should be able to detect if a significant amount of nuclear material has been removed from a spent fuel assembly and possibly replaced by dummies. According to the present safeguards criteria this target amount is half of the fuel pins. In addition, it would be important to minimise the probability of false alarms. One target of this task was to study whether it would be possible to draw conclusions from the measured data only, without making use of operator's declared data in the data analysis.

This task studied also the possible gain in fork performance, when a simultaneous gamma spectrometric measurement is performed. For this purpose an enhancement to a conventional fork detector (FDET) was made by adding a CdZnTe detector. Passive total neutron counts, gross gamma and gamma spectrometric measurements of intermediate resolution are simultaneously taken with this enhanced fork detector (EFDET).

Two measurement campaigns were performed at the Olkiluoto Interim Storage in 1999. Complete BWR assemblies were measured during these campaigns. The results of the measurements have been reported in ref. [1]. Complete VVER-440 assemblies were measured at the Loviisa Interim Storage in 2000. The results have been reported in ref. [2]. There was a possibility to measure incomplete spent fuel assemblies at the CLAB in 2001. The corresponding measurement results and model calculations have been presented in ref. [3]. Complementary model calculations have been presented in refs. [4] and [5].

This report is a summary of the measurements and model calculations performed under Task JNT A 1071 "Partial Defect Test on Spent Fuel LWRs". Additionally, the results of the MOX mock-up measurements performed at the SCK•CEN in 2001 are reported in this report. The basic hypothesis, which was under test in this study, is presented in section 2. Results of an earlier investigation performed at Los Alamos National Laboratory are reviewed in section 3. Section 4 concentrates on the measurements and model calculations. The conclusions are drawn in section 5.

## 2 Hypothesis of the fork method in partial defect verification

The  $^{137}\text{Cs}$  activity in an irradiated fuel assembly is known to depend linearly on the burnup:

$$G = k \cdot B. \quad (1)$$

Here  $G$  denotes the gamma emission rate produced by the  $^{137}\text{Cs}$  decay and  $B$  denotes the burnup.

Some of the transuranium isotopes produced during irradiation in the reactor emit neutrons through spontaneous fission. The principal neutron emitter is  $^{244}\text{Cm}$ . The relationship between the  $^{244}\text{Cm}$  activity and the burnup is not linear, but can be described as a power function of burnup, with the exponent value typically 4...5. The value of the exponent may depend on the reactor and fuel type and also on the irradiation conditions:

$$N = k' \cdot B^b, \quad (2)$$

where  $N$  denotes the neutron yield from spontaneous fission of  $^{244}\text{Cm}$ .

Combination of the equations (1) and (2) leads to a relationship between the  $^{137}\text{Cs}$  activity and

the emission rate of  $^{244}\text{Cm}$  neutrons:

$$N = k'' \cdot G^b, \quad (3)$$

where  $b$  is the above-mentioned exponent.

The idea of using a fork detector for partial defect verification originates from a hypothesis that neutrons and gamma rays give a different view of a spent fuel assembly. The highly penetrating neutrons give signal over the whole volume of the fuel assembly. Because of the strong self-absorption of gamma rays in uranium oxide fuel, the gamma rays detected outside the fuel assembly emanate predominantly from the surface of the fuel assembly. Therefore, the coefficient  $k''$  in equation (3) depends, among other things, on the geometrical configuration of the assembly. Also a partial defect affects this coefficient. A 50% defect is expected to give a neutron measurement result, which should be significantly below the correlation curve of complete assemblies. If this is found true, a partial defect test using a fork detector can be performed.

### 3 Earlier investigations

The possibility to reveal pin diversions with fork detector has been earlier investigated by Rinard and Bosler at the Los Alamos National Laboratory. The results, which are reported in ref. [6], are briefly reviewed in this section.

Calculations were performed for different pin removal configurations starting from a complete 15×15 PWR assembly with 204 pins. The calculations showed that the neutron count rate indicated the amount of removed material. In addition, the calculations implied that the gamma signal would depend on the pin removal geometry in the defected assembly. Removal of the pins from the centre of the assembly would not change the gamma signal, whereas a pin removal from the edge near the fork would reduce the gamma signal. However, experimental confirmation was not performed.

The investigation included also contemplation of different diversion strategies. It is a difficult task to successfully divert the nuclear material from a spent fuel assembly. Records may have to be falsified. Assemblies have to be moved without detection by a surveillance system. Fuel has to be removed from highly radioactive spent fuel assemblies. The defected assemblies have to be returned to the storage without being noticed. The integrity of the seals has to be maintained. In addition, the irregular assembly has to pass the partial defect verification without noticing.

If the cooling time and burnup are correctly declared, the probability that a diversion from a single assembly will be detected with fork detector depends on the position of the data point before the diversion, the size of the diversion and the

width of the normal distribution. The analysis implies that if 50% of the fuel pins were diverted from a few assemblies, it would be revealed with the fork detector. Owing to this a diverter would have to make small diversions from many assemblies to obtain a significant quantity of  $^{239}\text{Pu}$  or  $^{235}\text{U}$ . The relative amount of the diverted fuel pins from one assembly would have to be less than the width of the normal distribution. It would increase the possibility that the diversion will be detected by other safeguards activities e.g. surveillance cameras and seals. As a result a diverter might give up making a large diversion effort. The denial of the access to the fuel storage for inspections could also reveal diversion actions.

Use of the operator declared data was an essential part of the analysis of Rinard and Bosler. If the cooling time is falsified to be longer, somewhat larger diversions than in the case of correctly declared data could be made without detection in the first inspection measurement after the diversion. The diversion could be detected by a subsequent measurement. A false cooling time would have to match the operating history of the reactor. Declaring a false burnup would also allow little larger diversions compared to the case of correctly declared data. A carefully reduced burnup could conceal a reduced neutron count rate, but it would strongly affect the analysis of the gamma data. To control the gamma data also the cooling time could be altered. Owing to the increased detection probabilities connected to the falsely declared data, the diverter might choose to use the correctly declared data.

## 4 Experiments and model calculations

### 4.1 BWR and VVER spent fuel assemblies

A detailed description of the EFDET device used for the measurements can be found in ref. [1].

Twenty-six complete BWR assemblies were measured at the Olkiluoto Interim Storage and eighteen complete VVER assemblies at the Loviisa Interim Storage in Finland. A set of nine BWR assemblies with missing pins was measured at the CLAB interim storage facility in Oskarshamn in Sweden. Five of them had a nominal burnup of 18 MWd/kg. Four of those five assemblies were also modelled for their neutron and gamma yield using the Origen-S and MCNP-4C codes. Four complete BWR assemblies were measured at the CLAB facility to ensure about the compatibility with the Olkiluoto measurements.

Analysis methods were developed to improve the correlation of the measured neutron signal with the gamma signal. A detailed data analysis of the measurements is presented in refs. [1] and [2].

#### 4.1.1 CdZnTe enhancement

Table I lists the most prominent gamma-emitting nuclides found in irradiated fuel, see ref. [7]. From Table I one can see that, after a few years, the most important contributors to the gross gamma signal are  $^{137}\text{Cs}$ ,  $^{134}\text{Cs}$ ,  $^{106}\text{Ru/Rh}$ ,  $^{154}\text{Eu}$  and  $^{144}\text{Ce/Pr}$ .  $^{106}\text{Ru/Rh}$  activity was observed and corrected for only in one assembly having the shortest cooling time of all, 2.7 years. The activity of  $^{154}\text{Eu}$  at the evacuation is only a few per cent of the activity of  $^{137}\text{Cs}$ . Characteristic gamma peaks of  $^{154}\text{Eu}$  and  $^{144}\text{Ce/Pr}$  were not observed in the gamma spectrometric data.

The contribution of gamma emitting nuclides other than  $^{137}\text{Cs}$  was eliminated from the gross gamma signal using the gamma spectrometric data. The correction algorithm has been presented in detail in ref. [1]. The correction uses only the

activity ratios. They can be determined using the internal efficiency calibration of each measured spectrum as deduced from the multiple-peak  $^{134}\text{Cs}$  intensities following the algorithm of Gunnink [8]. Table I confirms that there are good grounds to assume that the corrected gross gamma signal is mainly due to the  $^{137}\text{Cs}$  activity. A cooling-time correction based on the physical half-life of  $^{137}\text{Cs}$  was applied to this corrected gross gamma signal. The application of these corrections was observed to improve significantly the quality of gross gamma data, i.e. the correlation of eq. (1) was improved. The assemblies with long cooling time, over 12 years, do not require any corrections to the gamma ray data. It can be assumed that the entire gross gamma signal is originating from  $^{137}\text{Cs}$ . For long-cooled assemblies additional gamma spectrometry, which is implemented in the EFDET, does not give any benefit. All assemblies subject to final disposal are expected to have a considerably longer cooling time than 12 years. This may not be valid for all assemblies subject to transfer into dry storages.

#### 4.1.2 Using the operator declared data

The operator declared data are needed in the data analysis. The initial enrichment, burnup and cooling time are needed for calculating the share of  $^{244}\text{Cm}$  neutrons in the measured neutron signal. The net  $^{244}\text{Cm}$  count rate value is corrected for decay to give the count rate at the evacuation date. The neutron signal was additionally corrected to bring all assemblies into one correlation curve corresponding to the reference enrichment of 2.95%. Data about possible off-reactor cycles are needed for off-reactor correction of the gross gamma signal and neutron signal. [2]

As pointed out already in ref. [6] the application of the above-mentioned corrections are essential for reducing the scattering of measured data.



**Table I.** Principal nuclides that can be detected in nuclear fuel by gamma spectrometry. [7]

Nuclide	Half-life	Principal gamma rays		Thermal fission mass yield		
		Energy (keV)	Branching (%)	<sup>233</sup> U	<sup>235</sup> U	<sup>239</sup> Pu
<sup>95</sup> Nb	34.975 d	765.8	100	6.3	6.50	4.81
<sup>95</sup> Zr	64.02 d	235.7 724.2 756.7	0.3 44.0 54.0			
<sup>103</sup> Ru	39.26 d	497.1 610.3	91.0 6.8	1.57	3.03	7.0
<sup>106</sup> Ru→ <sup>106</sup> Rh <sup>(*)</sup>	373.59 d	511.8 621.9 1050.4 1128 1562.2	20.0 10.0 1.6 0.4 0.2	0.25	0.401	4.3
<sup>134</sup> Cs	2.065 a	563.2 569.3 604.7 795.9 802 1365.2	8.4 15.0 98.0 86.0 8.7 3.0	6.30	6.87	7.68
<sup>137</sup> Cs	30.07 a	661.7	85.0	6.81	6.19	6.62
<sup>140</sup> Ba→ <sup>140</sup> La <sup>(*)</sup>	12.752 d	815.8 925.2 1596.2 2521.4	23.0 6.9 95.0 3.5	6.4	6.21	5.38
<sup>144</sup> Ce→ <sup>145</sup> Pr <sup>(*)</sup>	284.893 d	696.5 1489.2 2185.7	1.3 0.3 0.7	4.68	5.50	3.74
<sup>154</sup> Eu	8.593 a	591.8 723.3 873.2 996.3 1004.7 1274.4	5.0 20.0 12.0 11.0 18.0 35.0	0.047	0.074	0.262

(\*) The half-lives for <sup>106</sup>Rh, <sup>140</sup>La, and <sup>144</sup>Pr are 29.80 seconds, 1.6781 days and 17.28 minutes, respectively.

#### 4.1.3 Error sources

The fission and ionisation chambers are placed in such a way that the horizontal positioning errors to these signals should be minimized. Gamma spectrometric data are sensitive to the variation of the actual distance of the fuel assembly from the CZT detector. The correction for parasitic gamma rays to the gross gamma signal uses only activity ratios of nuclides. This means that the correction for the short-lived gamma emitters is practically independent of the horizontal positioning error. In fact, the observed <sup>134</sup>Cs/<sup>137</sup>Cs activity ratio was almost constant independent of the lateral positioning or the azimuth angle. This is expected to be

valid also for other activity ratios.

The assemblies were measured at all four sides in Olkiluoto and at two azimuth angles of 120° interval in Loviisa. At the CLAB facility the measurements were taken on three sides of the assembly. The fourth side was inaccessible for technical reasons. The data taken of each assembly were averaged over all sides measured. The <sup>244</sup>Cm neutron counts were correlated to the gross gamma according to equation (3) using the averaged and non-averaged data. Averaging did not change the width of the obtained error corridor. This implies that the random factors attributed to the measurement itself, like positioning accuracy and

counting statistics, do not significantly affect the accuracy of an individual measurement. It can be concluded that the width of the error corridor is predominantly determined by variation of uncontrolled factors like local conditions during irradiation. Also the declared burnup, needed in the corrections to the measured data, contain errors. These factors have not been taken into consideration in the analysis. The error source contemplations presented in ref. [6] have lead to similar conclusions.

A factor specifically attributed to the irradiation conditions of BWRs is the void fraction. The void fraction depends on the position of the assembly in the core. Interesting cases are those assemblies, which have low evacuation burnup, either due to having been irradiated in the initial operating cycles or due to some incident, e.g. leak, causing their early evacuation. Due to radial distribution of the void fraction those assemblies may have effective void fraction over their irradiation history different from that of high burnup assemblies. This may induce additional fluctuation of the data points at low burnup.

Some of the incomplete assemblies measured at the CLAB were reconstituted. Those assemblies had pins of different cooling times and different irradiation histories and they bring additional error to the analysis of the CLAB data.

The measurements were performed at three different vertical levels in Olkiluoto and in Loviisa: at the mid-point, 500 mm above the mid point and 500 mm below the mid-point.  $^{244}\text{Cm}$  neutron counts were correlated with gross gamma using the data measured at the mid-point. Also the corresponding data points of the lower and higher heights were found to be inside of the error corridor of the mid-point curve. It implies that the burnup profile variation and positioning in axial direction are not a significant error source at least within one metre interval in the centre of an assembly.

#### 4.1.4 Neutron versus burnup correlation

In case the operator's data are available and considered reliable, the partial defect verification of spent fuel could be performed utilizing the correlation between the  $^{244}\text{Cm}$  neutron yield and the declared burnup according to eq. (2). Figure 1 shows this plot for all measured BWR assemblies.

[1, 3] All neutron versus burnup or neutron versus gross gamma plots are displayed in a log–log scale, as in this scale the power function is displayed as a straight line with the slope equal to the exponent. E.g. eq. (2) transforms into

$$\log N = b \log B + \log k' \quad (4)$$

The curve has been fitted using the neutron yield measurements of the complete assemblies. The value obtained to the exponent  $b$  is  $4.44 \pm 0.09$ . The width of the 90% error corridor is  $\pm 22\%$ . This corresponds to an error of 5% in burnup determination from the neutron yield. This is in accordance with the general assumption that the operator declared burnup values should be correct within 5%. Subsequently the error corridor of 90% confidence level is used throughout this report. The 90% error corridor is defined so that statistically 90% of individual measurements should fall within this corridor, 5% above and 5% below this corridor.

For incomplete assemblies of very low burnup, 8 and 11 MWd/kg, the defect could not be verified. They exhibit even higher neutron yield than could be anticipated even if the two assemblies with burnup of 11 MWd/kg have about 30% of pins missing. At low burnup the proportion of the  $^{244}\text{Cm}$  neutrons of the total neutron yield is low, which signifies that a fairly large correction has to be made to the experimental neutron rate. This large correction is subject to errors and inaccuracies of the codes used and of the nuclear data embedded

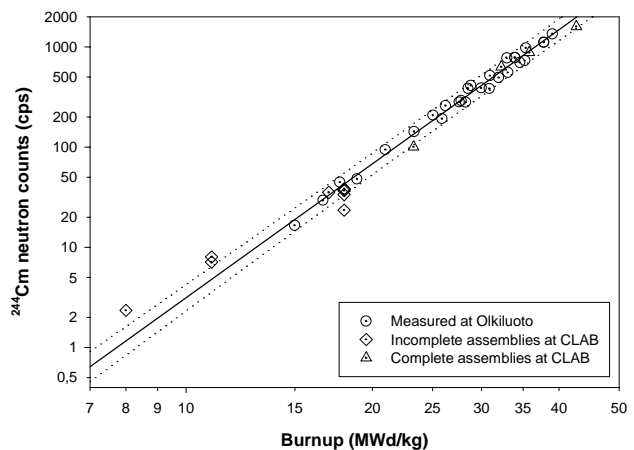


**Figure 1.** Neutron versus burnup curve for spent BWR fuel assemblies. The dotted lines describe the error corridor. One assembly with BU=18 MWd/kg and 35% of pins missing falls clearly below the error corridor.

in those codes. This makes the interpretation of the measured neutron yield of very low burnup assemblies quite difficult.

The effect of missing pins is clearly seen in the series of incomplete assemblies of burnup equal to 18 MWd/kg. From those assemblies the one with 65% of the pins left falls clearly below the error corridor indicating that a defect of 35% or larger would be detected for assemblies with burnup of 18 MWd/kg, see Figure 1. By interpolation, the limit value of detection of missing pins using neutron versus burnup correlation could be estimated as 21% of pins missing at 18 MWd/kg at a 95% confidence level. The effect is stronger and the verification should be easier for higher burnup assemblies.

Figure 2 shows the neutron versus burnup correlation for the VVER-440 assemblies measured at the Loviisa NPP. [2] The experimental exponent value obtained is  $b = 5.18 \pm 0.10$ . The width of the error corridor is  $\pm 34\%$ . This corresponds to an error of 6.6% in burnup determination from the neutron yield. This is somewhat higher than in the case of BWR.

#### 4.1.5 Neutron versus gamma correlation

The original target of the task was to find out whether it would be possible to apply fork data for partial defect verification without using the operator's data. In the first place it is evident that the cooling-time correction is necessary to bring the measured data to a reference date. Therefore the

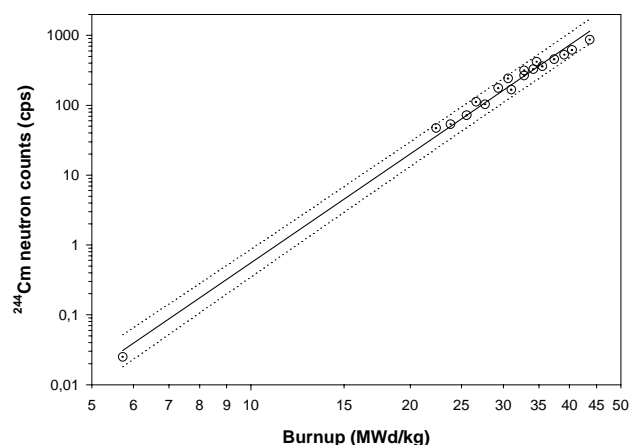


**Figure 2.** Neutron versus burnup curve as measured for VVER-440 assemblies at Loviisa NPP.

use of operator's data is always unavoidable in order to make the measurements of different assemblies comparable to one correlation curve.

If only cooling-time is available and considered reliable, the gross gamma data can be corrected to reduce the scattering using only the gamma spectrometric data and the known cooling times. Figure 3 displays the gross gamma versus burnup correlation according to eq. (1), obtained experimentally for BWR assemblies based on the Olkiluoto data. It can be deduced from the statistical analysis that the gross gamma signal can determine a burnup at an accuracy  $\pm 2.9$  MWd/kg at the 90% confidence level for BU=14–40 MWd/kg. Also one can see that the gross gamma signals of the complete assemblies measured at the CLAB are in agreement with the correlation curve deduced from the Olkiluoto data. The incomplete assemblies of BU=17–18 MWd/kg show a clear reduction of the gross gamma signal. This is due to the configuration of the missing pins, as the missing pins were predominantly taken from the outer rows and columns of the assembly. This configuration dependence of the gamma signal is further contemplated in section 4.2, where the results of the experiments made with a fresh MOX mock-up performed at the SCK•CEN in Mol are reported.

If the neutron versus burnup correlation is combined with the burnup versus gross gamma correlation, the scattering of the data points is, of course higher than that of the neutron versus burnup correlation only. Figure 4 displays the

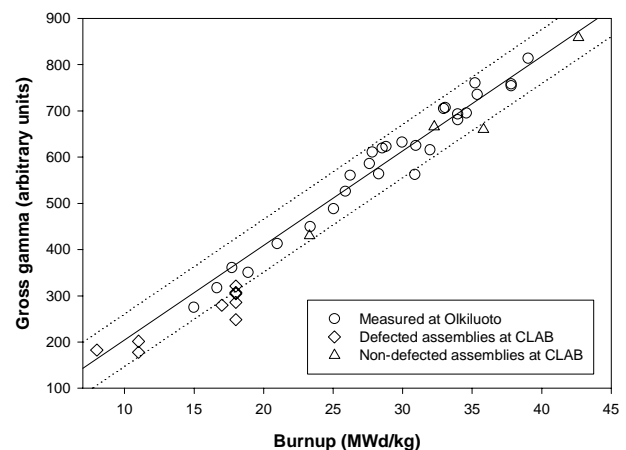


**Figure 3.** Gross gamma signal versus burnup of BWR assemblies. The curve fitting was made to the Olkiluoto data only. The dotted lines describe the error corridor.

measurement results of the BWR spent fuel assemblies according to the correlation expressed in eq. (3). The corrections as described in section 4.1.2, based on the use of the operator's data, are applied. The width of the resulting error corridor is  $\pm 31\%$ .

The amount of pins left in the incomplete BWR assemblies ranged between 65% and 94%. None of these pin configurations hit below the lower limit of the error corridor of the neutron versus gross gamma curve. Some incomplete assemblies have the data point even above the upper limit of the error corridor. The investigations show that both the neutron and the gamma signal depend on the amount of the fuel left in the assembly. In addition, the gamma signal has a strong configuration dependence of the incomplete assemblies. Mainly this configuration dependence makes the application of the neutron versus gross gamma correlation for partial defect verification impossible. In making this conclusion it is assumed that the actual configuration of the incomplete assemblies cannot be verified in any other method, thus making it impossible to take it into account in the data evaluation.

Although incomplete VVER-440 assemblies were not available it can be concluded based on the general behaviour of the complete VVER assemblies that partial defect verification is possible based on reliable operator's data on the burnup and cooling time, at least for the assemblies of high burnup. However, the use of neutrons versus gross gamma correlation for partial defect verification would be impossible also for VVER-440 assemblies.

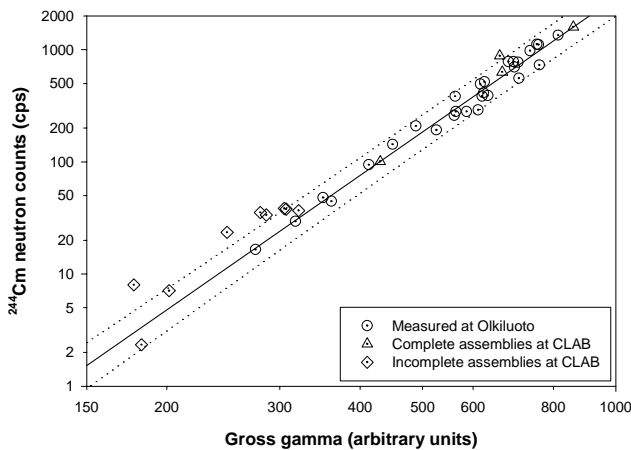


**Figure 4.** Neutrons versus gross gamma signal curve for the BWR spent fuel assemblies. The dotted lines describe the error corridor.

#### 4.1.6 Model calculations

Model calculations with Origen-S and Monte Carlo code MCNP-4C were performed to investigate the radiation fields around a defected BWR 8x8 fuel assembly. The results have been reported in refs. [4] and [5]. The calculations for the four incomplete assemblies with missing pins, which also were measured at the CLAB, showed quite similar behaviour as the measurement results.

Varying number of fuel pins was removed to find out to what extent the number of removed pins affects the radiation fields. Also the effect of different removal configurations was investigated. The replacement scenario was studied, as well. In the replacement scenario the removed fuel pins were replaced by lead pins to compensate for the mass reduction. Figure 5 displays the calculated neutron yield versus the relative mass in the removal scenario without pin replacement. [5] An almost linear dependence of the neutron yield is found. The fit to a second order curve, which intersects the point (1,1),

$$N_{rel} = a \cdot m_{rel} + (1 - a) \cdot m_{rel}^2 \quad (5)$$

gives a value  $a = 0.68 \pm 0.02$  for the relative mass range  $0.5 < m_{rel} < 1.0$ . An equal value was obtained in ref. [5] for the replacement scenario implying that the replacement of the removed rods with dummies has practically no effect to the neutron yield.

Figure 6 displays the calculated relative neutron yield plotted into the scaled experimental calibration curve of Figure 1. From the calculations, using the error corridor of Figure 1, the limit

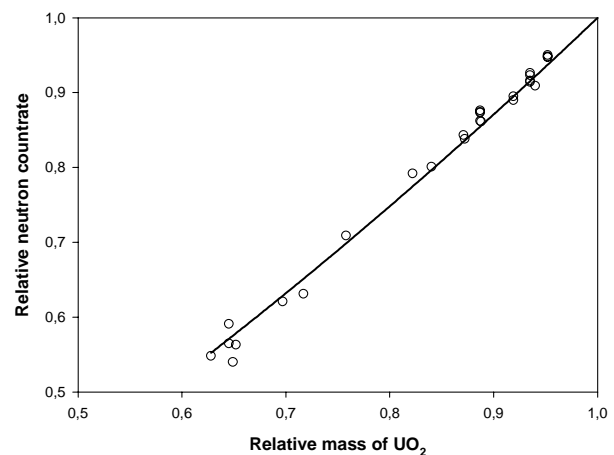


**Figure 5.** Calculated neutron yield as a function of the relative fissile mass of the fuel assembly.

value of detection of defect could be estimated as 19% at 90% confidence level. This is in good accordance with the experimental value of 21%.

Figure 7 shows a situation where the measured  $^{244}\text{Cm}$  neutron and  $^{137}\text{Cs}$  gamma yield would be available but the operator's burnup data would be unavailable or unreliable. Figure 7 is analogous with Figure 4 using the data from model calculations instead of experimental data. The data are scaled so that the calibration curve and the error corridor could be plotted in the same plot. Figure 7 shows that almost all cases of incomplete assemblies, which were modelled in ref. [5], would fall between the limits of the error corridor. Those two falling outside the error corridor are lying above its upper limit. This is due to the fact that in those cases the reduction of the gamma signal overbalances that of the neutron signal. This is another manifestation of a strong configuration dependence of the gamma signal. It also confirms the conclusion drawn in section 4.1.5 that partial defect verification based on the measured neutron and gamma signals only is not possible in a general case.

## 4.2 Mock-up assemblies

Pin configurations of real spent fuel assemblies cannot be arranged just for the purpose of testing the partial defect. Practically the only way to perform the experiment with arbitrary pin configurations is by measuring a mock-up assembly.

There is a fresh MOX mock-up assembly available at the VENUS experimental facility of the SCK•CEN in Belgium. This allows the realization

of any pin configuration both for a 9×9 BWR and for a 17×17 PWR mock-up fuel. An experiment was performed at the SCK•CEN in order to obtain experimental confirmation of the partial defect test capability of the fork detector [9].

The mock-up assembly was placed into a standard measurement position between the fork prongs. A standard fork detector was modified for the experiment with fresh MOX fuel. The fission neutrons of plutonium represented the spontaneous fission neutrons of  $^{244}\text{Cm}$ . The four fission chambers of the standard fork detector were replaced by two  $^3\text{He}$  counters to increase the neutron sensitivity. To obtain higher sensitivity for detection of gamma rays emitted by the plutonium and americium isotopes present in fresh MOX fuel, the fork included four ionisation chambers instead of two.

The gamma spectrum of fresh MOX fuel is different from that of spent LWR fuel. It is assumed that although the attenuation of the MOX gamma rays in the fuel pins and in water differs from that of a spent fuel assembly, the general behaviour should be similar enough. This would allow drawing conclusions about the configuration dependence of the spent fuel gamma radiation from the results obtained from the MOX mock-up.

### 4.2.1 BWR mock-up assembly

The measurements were performed in water. The BWR mock-up assembly used in the measurements was a 9×9 grid with fresh MOX fuel pins. The measured defect geometries are presented in Annex 1. The measured data are presented in An-

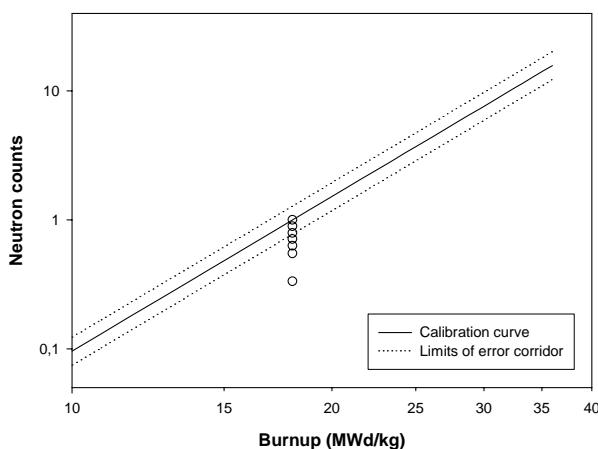


**Figure 6.** Calculated effect of the removal of pins for an assembly of burnup = 18 MWd/kg. The calculated points are plotted in an experimental calibration curve with the error corridor indicated.

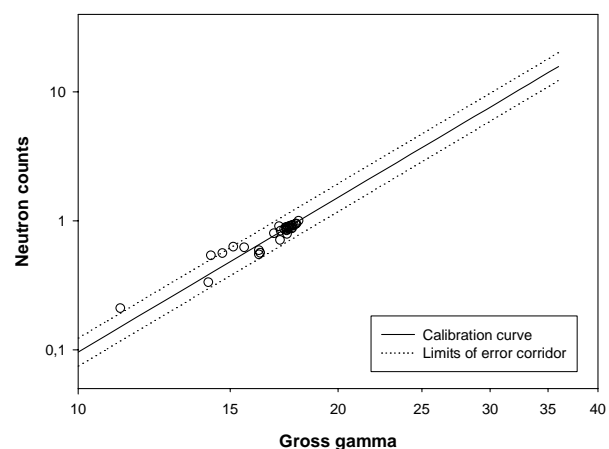


**Figure 7.** The calculated  $^{244}\text{Cm}$  neutrons versus  $^{137}\text{Cs}$  gamma yield of incomplete assemblies of burnup = 18 MWd/kg [5] as plotted together with the experimental calibration curve.

nex 2.

The measured neutron and gamma data have been plotted in Figure 8. The data taken from the complete  $9 \times 9 - 1$  configurations have been averaged. This average value was used as the reference point. The measured neutron and gamma data have been scaled by dividing with the corresponding values of the reference point. A reference curve is a power curve with the exponent 4.44, which goes through the reference point with  $\pm 22\%$  error corridors. Measurement of a set of non-defected assemblies with variable burnup is expected to give readings falling inside the displayed error corridor.

The series, where central rods were removed (see Figure 8), show systematic drop of the neutron signal, which overbalances the drop of the gamma signal in such a way that the neutron signal finally drops below the lower limit of the error corridor. The same applies to the case, where columns parallel to the fork prongs are returned starting from the column closest to the detector. These cases confirm that the vast majority of the gross gamma signal emanates from the columns closest to the detector prongs. In all other removal patterns the drop of the gamma signal overbalances the drop of the neutron count rate in such a way that there is a tendency of finding the measurement point above the correlation curve of complete assemblies. It is not too difficult to find removal patterns where the measured signals fall inside

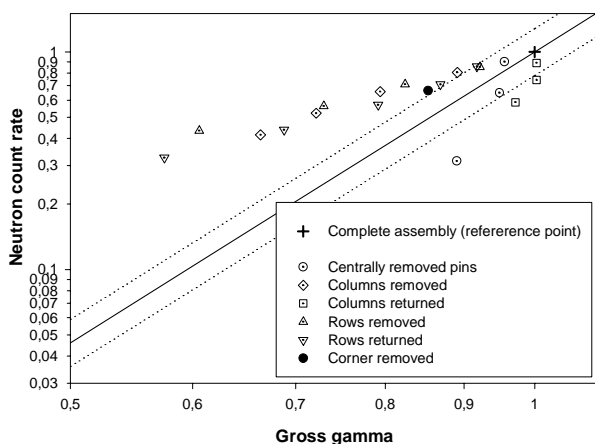


**Figure 8.** Measured neutron signal versus gross gamma signal in different defect configurations. The cross is the average value of the measured data points of a complete  $9 \times 9 - 1$  geometry as scaled to the point (1,1). Solid curve is the correlation curve of complete assemblies and dotted lines describe the error corridor.

the error corridor of complete assemblies. This is manifested in Figure 6 where the majority of configurations modelled give neutron and gamma signals that fall inside the error corridor.

#### 4.2.2 PWR mock-up assembly

The measurements of the  $17 \times 17$  PWR grid were performed in borated water (2270 ppm). The complete PWR mock-up assembly was a  $17 \times 17 - 25$  configuration with 264 fresh MOX pins and 25 open channels [9].

The corresponding analysis as described in section 4.2.1 was made to the data of PWR mock-up assembly. The configurations are displayed in Annex 3 and the measured data are shown in Annex 4. A neutron versus gross gamma plot of the measured configurations is displayed in Figure 9 together with a scaled correlation curve with the  $\pm 22\%$  error corridor indicated. Again the measured configurations scatter predominantly inside the error corridor of the correlation curve with the exponent equal to 4.44 (the exact value is immaterial). When the pin columns close to the left prong were removed the data points rise above error corridor. This again manifests that the removal of columns nearest to the sensors induces a drop of the gamma signal that overbalances the drop of the neutron signal. This allows an intelligent diverter to devise such pin configurations of a PWR assembly that can pass verification based on the neutron versus gross gamma correlation.

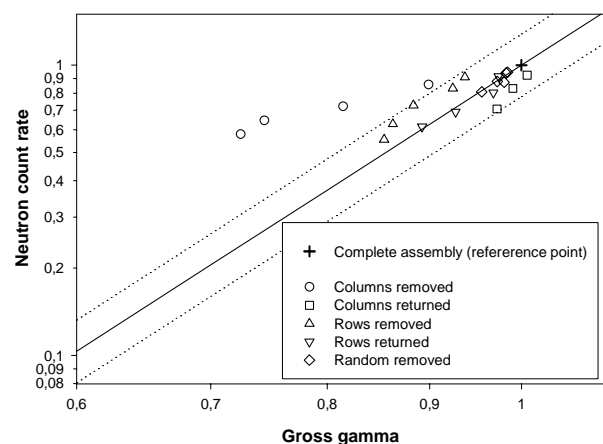


**Figure 9.** Measured neutron versus gross gamma in the MOX mock-up in a  $17 \times 17$  PWR configuration. The results have been plotted into a correlation curve with the exponent 4.44, which is scaled so that the average yield of complete configurations falls into the point (1,1).

## 5 Conclusion

Both the neutron and the gamma signal depend on the amount of the fuel left in the assembly. As expected, the neutron signal decreases almost linearly with the amount of fuel pins removed quite independently of the removal geometry. The gamma signal depends strongly on the pin configuration of incomplete assemblies. If the row closest to the ionisation chamber remains full, the gross gamma signal does not significantly decrease as the pins are removed. If the pins close to the detectors are removed, the gross gamma signal decreases significantly. As a result there exist configurations even with 50% of removed pins, which cannot be detected using the neutron versus gross gamma curve.

For short-cooled assemblies, 3–12 years, the use of spectrometric data of EFDET can be utilised for elimination of contribution of short-lived nuclides, mainly  $^{134}\text{Cs}$  and sometimes also  $^{106}\text{Ru}/\text{Rh}$ . This correction allows the application of the physical half-life of  $^{137}\text{Cs}$  in the cooling-time correction of the gross gamma signal. For assemblies of cooling-time longer than 12 years, the physical half-life of  $^{137}\text{Cs}$  is directly applicable for the cooling-time correction. For these long-cooled assemblies gamma spectroscopy does not give any improvement to the data quality.

The fork measurements, either with a FDET or EFDET device, cannot be applied for partial defect test without use of the operator declared data. This gives additional possibilities to cover a nuclear material diversion by falsifying the data declared by the operator. For this reason it is very important to maintain the continuity of knowledge by keeping an up-to-date database of the irradiation histories of the fuel assemblies starting from the date when each assembly is inserted into the reactor for the first time. In this way it would be very difficult for the operator to manipulate later the irradiation data for dishonest purposes.

When an up-to-date database exists, a consistency-check of the burnup and other irradiation history data could be applied using the gross gamma data. In this case the neutron versus burnup curve could be utilised for partial defect verification purposes. A removal of about 20% or more of the pins would be detected at a 95% confidence level for assemblies of burnup 18 MWd/kg or higher.

For developing a reliable, operator data independent partial defect verification device a totally different approach must be applied.

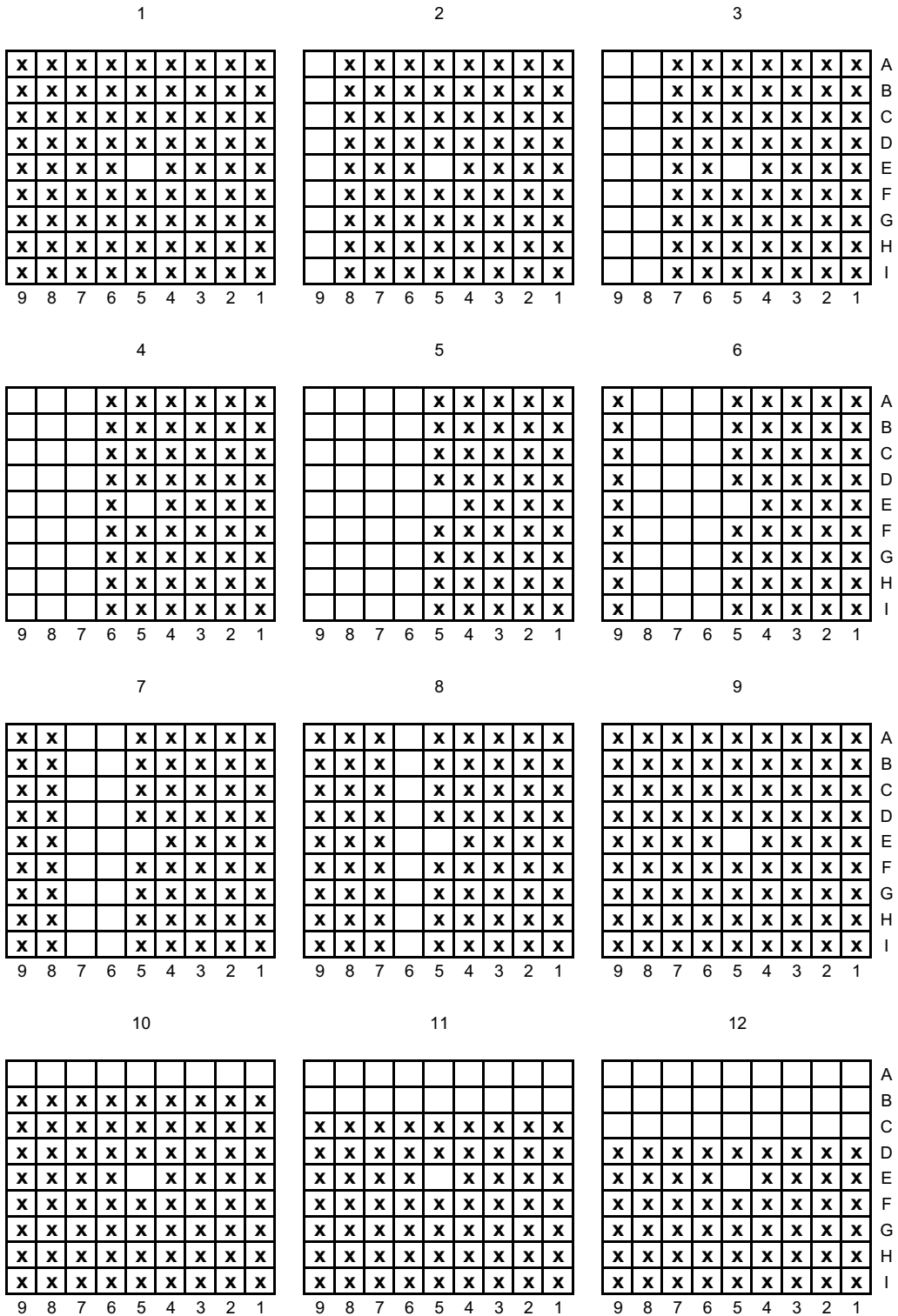
## References

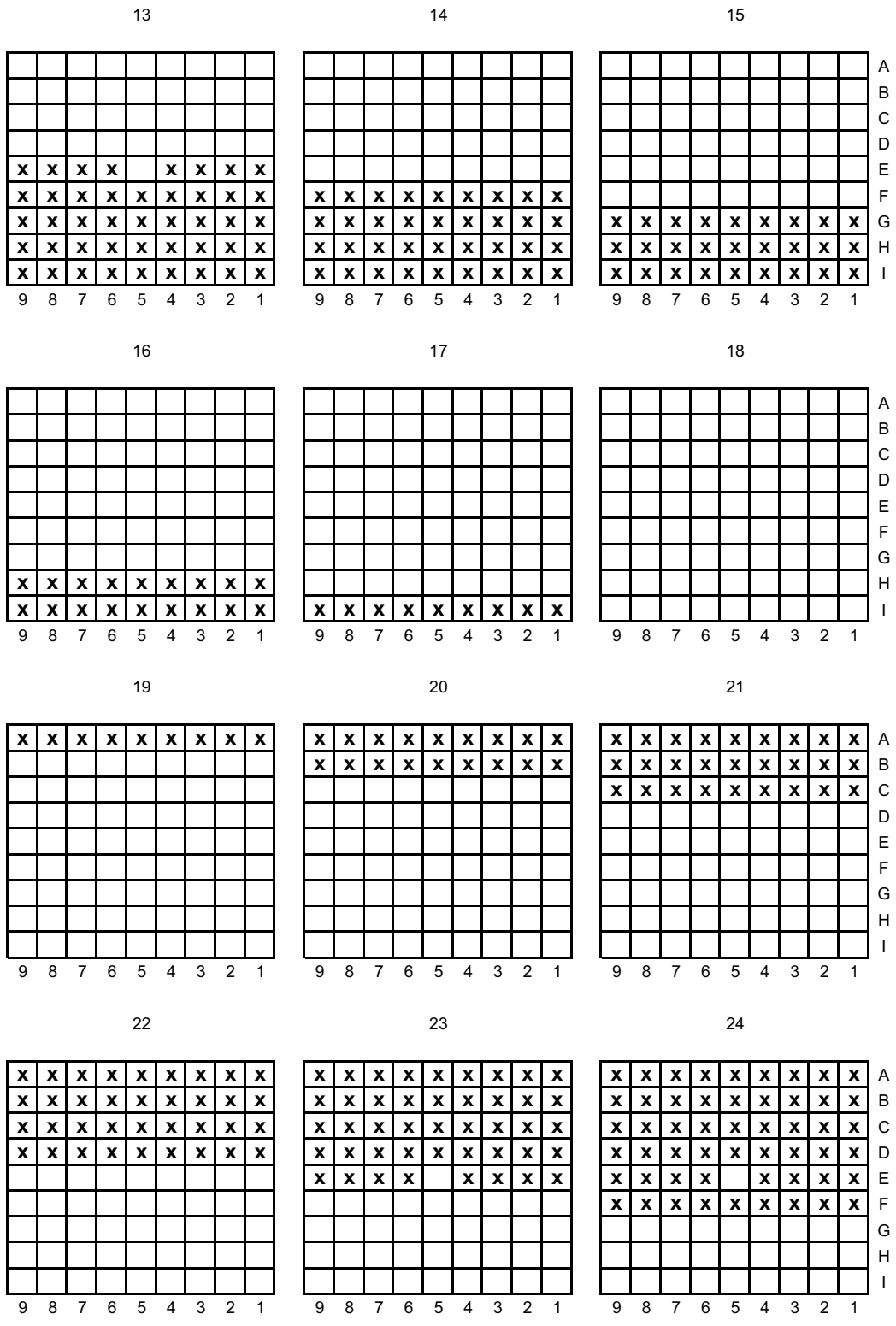
1. Tiitta A, Hautamäki J, Turunen A, Arlt R, Arenas Carrasco J, Esmailpour-Kazerouni K, Schwalbach P. Spent BWR fuel characterisation combining a fork detector with gamma spectrometry. Report STUK-YTO-TR 175, Radiation and Nuclear Safety Authority, Helsinki (2001).
2. Tiitta A, Hautamäki J. Spent VVER fuel characterisation combining a fork detector with gamma spectrometry. Report STUK-YTO-TR 181, Radiation and Nuclear Safety Authority, Helsinki (2001).
3. Tiitta A, Saarinen J, Tarvainen M, Jansson P, Håkansson A, Jansson K. Enhanced fork detector for partial defect verification of BWR fuel assemblies. Paper IAEA-SM-367/14/02 in Proceedings of the Symposium on International Safeguards, IAEA, Vienna, 2001.
4. Jansson P, Håkansson A, Bäcklin A. Neutronic effects of partial defects in BWR 8x8 spent fuel assemblies. Uppsala University, Dept. of Radiation Sciences, Nuclear Technology 2002 (submitted).
5. Jansson P, Håkansson A, Bäcklin A. Detection of partial defects in irradiated BWR fuel assemblies. A preliminary study. Presented at the 43<sup>rd</sup> INMM Annual Meeting, June 23–27, 2002.
6. Rinard PM, Bosler GE. Safeguarding LWR Spent Fuel with the Fork Detector. LA-11096-MS, Los Alamos (1988).
7. Jansson P. Studies of nuclear fuel by means of nuclear spectroscopic methods. PhD Dissertation. Comprehensive summaries of Uppsala dissertations from the Faculty of Science and Technology 714. Uppsala Universitet, Uppsala, 2002.
8. Gunnink R. A Guide Using Cs Ratio, PC version 1.1 for DOS and Windows. December 1998.
9. Carchon R, Bruggeman M, Koulikov Y, Lee YG, De Baere P. Measurement of Fresh MOX-LWR Fuel Assemblies with the IAEA-Fork Detectors – Calibration of IAEA PWR and BWR UWCC, SCK•CEN report R-3614, April 2002.



# ANNEX 1 MEASURED DEFECT GEOMETRIES OF THE MOX MOCK-UP ASSEMBLY IN BWR 9×9–1 GEOMETRY

The configurations measured for the BWR mock-up. Configurations 1, 9 and 27 are complete assemblies. The fork prongs containing the neutron and gamma sensors were placed in parallel with the columns.







## ANNEX 2 THE MEASURED DATA, BWR MOCK-UP ASSEMBLY

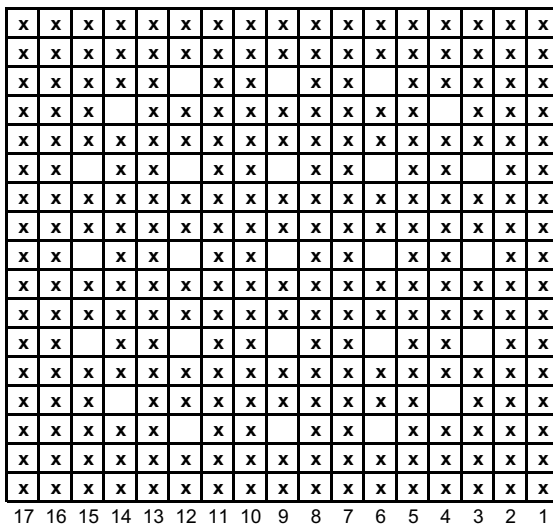
G1 represents an average of the left prong gamma reading from three measurements. Because the gamma signal of the right prong was not reliable, the reading of the right prong was assumed equal to that of the left prong in symmetrical geometries (1, 9–30). In non-symmetrical geometries (2–8, 31) the gamma reading of the right prong was assumed equal to that of the left prong at full configuration. G total is the sum of the gamma readings of the left (measured) and the right (deduced on the basis of symmetry) prong.

No. of configuration	Pins left	Pins left (%)	G1	G total	N total (cps)	Sdev of N total (cps)	Description
1	80	100,00	0,03262	0,06374	2404,87	8,95	Complete
2	71	88,75	0,02438	0,05550	1949,17	8,06	Removed column 9
3	62	77,50	0,01869	0,04982	1590,66	7,28	Removed columns 9, 8
4	53	66,25	0,01446	0,04558	1264,87	6,58	Removed columns 9, 8, 7
5	44	55,00	0,01109	0,04221	1005,53	5,84	Removed columns 9, 8, 7, 6
6	53	66,25	0,02911	0,06024	1419,51	6,96	Removed columns 8, 7, 6
7	62	77,50	0,03094	0,06207	1799,40	7,92	Removed columns 7, 6
8	71	88,75	0,03093	0,06205	2156,05	8,60	Removed column 6
9	80	100,00	0,03117	0,06229	2406,44	9,12	Complete
9	80	100,00	0,03104	0,06216			Repeat
10	71	88,75	0,02848	0,05697	2062,52	8,44	Removed row A
11	62	77,50	0,02562	0,05125	1717,91	7,65	Removed rows A, B
12	53	66,25	0,02286	0,04573	1365,26	6,83	Removed rows A–C
13	44	55,00	0,01923	0,03846	1052,13	5,92	Removed rows A–D
14	36	45,00	0,01591	0,03182	780,69	5,16	Removed rows A–E
15	27	33,75	0,01232	0,02465	531,75	4,25	Removed rows A–F
16	18	22,50	0,00967	0,01933	320,28	3,28	Removed rows A–G
17	9	11,25	0,00694	0,01389	138,68	2,16	Removed rows A–H
18	0	0,00	0,00147	0,00294	0,30	0,10	Empty (background)
19	9	11,25	0,00806	0,01613	138,35	2,17	Removed rows B–I
20	18	22,50	0,01189	0,02378	314,08	3,25	Removed rows C–I
21	27	33,75	0,01473	0,02946	536,62	4,27	Removed rows D–I
22	36	45,00	0,01833	0,03666	790,30	5,17	Removed rows E–I
23	44	55,00	0,02163	0,04327	1061,31	5,99	Removed rows F–I
24	53	66,25	0,02467	0,04935	1381,70	6,87	Removed rows G–I
25	62	77,50	0,02693	0,05387	1715,98	7,68	Removed rows H, I
26	71	88,75	0,02836	0,05672	2074,33	8,53	Removed row I
27	80	100,00	0,02966	0,05932	2435,58	9,18	Complete
28	72	90,00	0,02949	0,05898	2180,10	8,71	Removed central rods 3×3
29	56	70,00	0,02928	0,05856	1569,38	7,38	Removed central rods 5×5
30	32	40,00	0,02756	0,05512	761,67	5,08	Removed central rods 7×7
31	60	75,00	0,02149	0,05262	1604,36	7,40	Removed down left corner 5×4

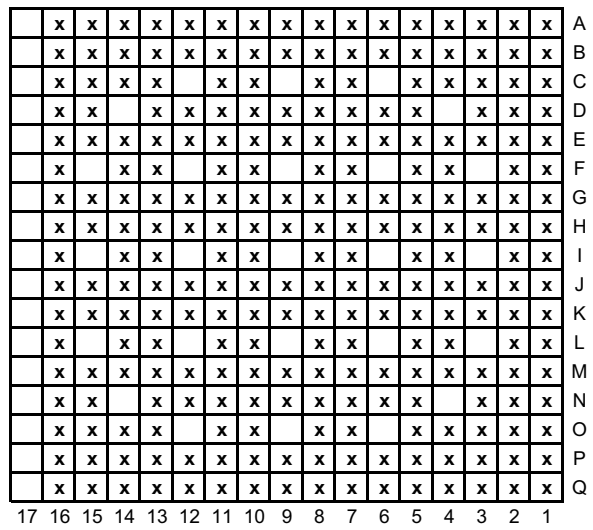
# ANNEX 3 MEASURED DEFECT GEOMETRIES, MOX MOCK-UP ASSEMBLY IN PWR 17×17–25 GEOMETRY

The configurations measured for the PWR mock-up. Configurations 32, 40, 50 and 56 are complete assemblies. The fork prongs containing the neutron and gamma sensors were placed in parallel with the columns.

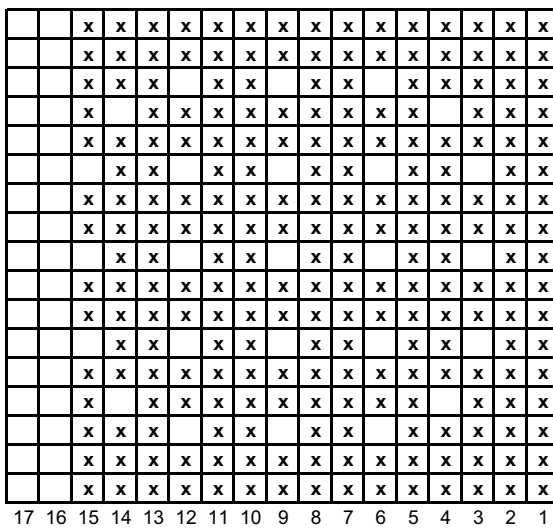
32



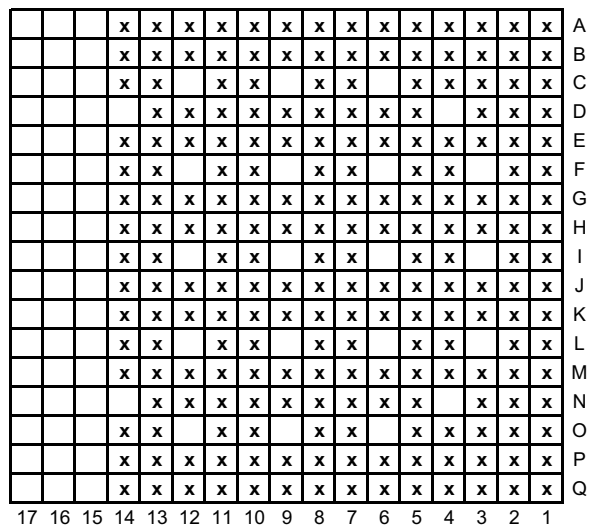
33



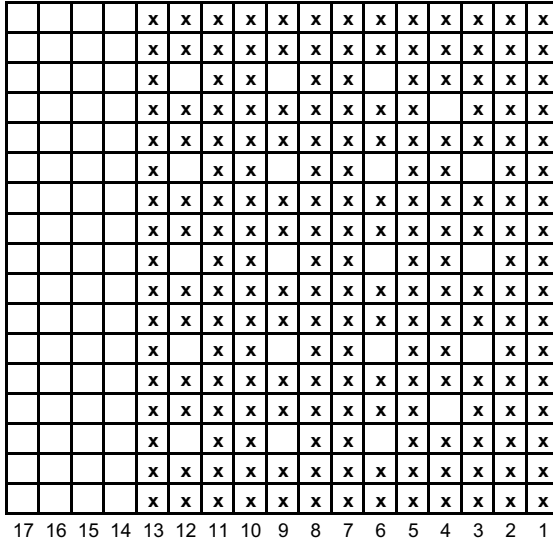
34



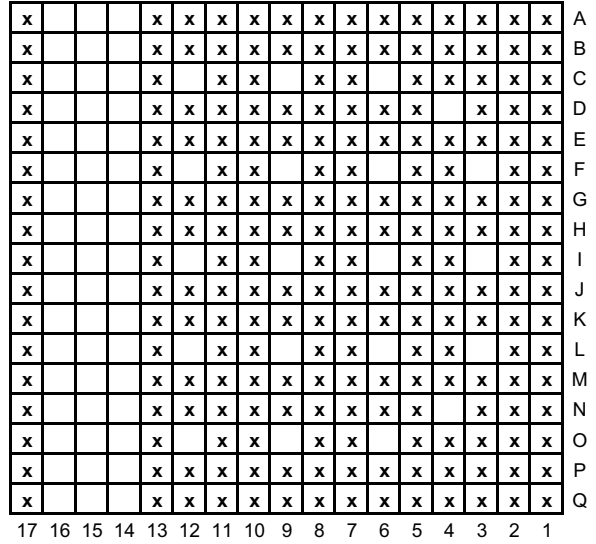
35



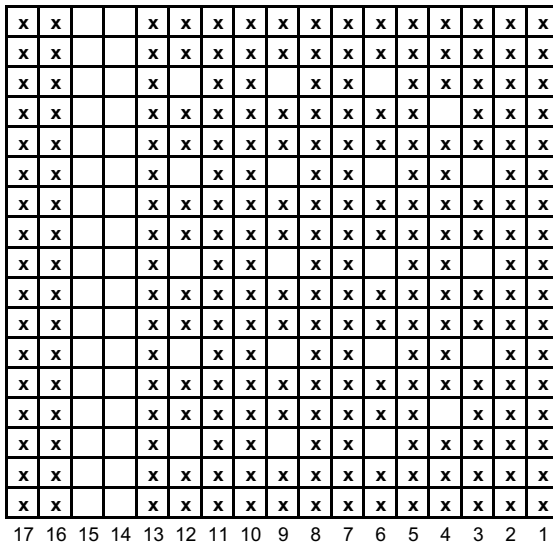
36



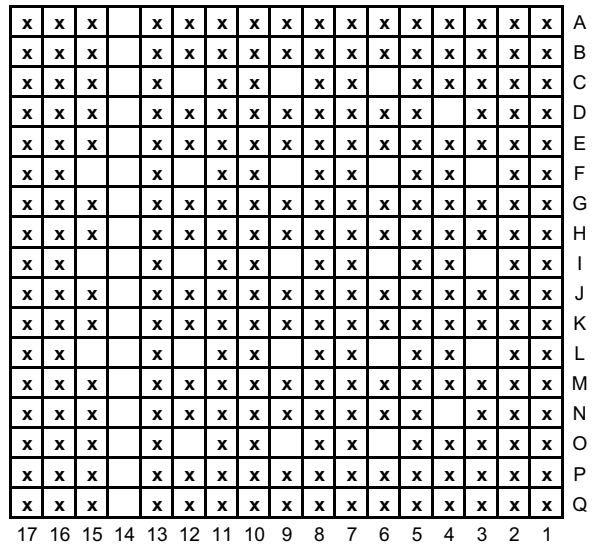
37



38



39













## ANNEX 4 THE MEASURED DATA, PWR MOCK-UP ASSEMBLY

G1 and G2 are average values of three gamma measurements, referring to the left and right prong correspondingly. G total is the sum of G1 and G2. The random groups A, B, and C refer to the randomly selected groups of 13 rods listed below.

No. of configuration	Pins left	Pins left (%)	G1	G2	G total	N total (cps)	Sdev of N total (cps)	Description
32	264	100,00	0,044180	0,043073	0,087253	3038,23	10,22	Complete
33	247	93,56	0,035963	0,043163	0,079127	2657,36	9,53	Removed column 17
34	230	87,12	0,028653	0,043100	0,071753	2236,92	8,76	Removed column 17, 16
35	216	81,82	0,023453	0,042097	0,065550	2000,89	8,26	Removed column 17–15
36	201	76,14	0,019903	0,043877	0,063780	1796,03	7,84	Removed column 17–14
37	218	82,58	0,042557	0,043050	0,085607	2195,16	8,67	Removed column 16–14
38	235	89,02	0,043800	0,043380	0,087180	2579,68	9,41	Removed column 15, 14
39	249	94,32	0,044460	0,044160	0,088620	2867,49	9,84	Removed column 14
40	264	100,00	0,044013	0,043200	0,087213	3142,21	10,40	Complete
41	247	93,56	0,041483	0,041030	0,082513	2825,93	9,85	Removed row A
42	233	88,26	0,040680	0,040687	0,081367	2583,86	9,37	Removed rows A, C
43	216	81,82	0,039450	0,038317	0,077767	2257,21	8,78	Removed rows A, C, E
44	199	75,38	0,038790	0,037160	0,075950	1946,34	8,12	Removed rows A, C, E, G
45	187	70,83	0,037927	0,037263	0,075190	1722,83	7,65	Removed rows A, C, E, G, I
46	204	77,27	0,040213	0,038333	0,078547	1907,89	8,03	Removed rows C, E, G, I,
47	218	82,58	0,041497	0,040137	0,081633	2142,00	8,51	Removed rows E, G, I,
48	235	89,02	0,042837	0,042400	0,085237	2493,48	9,22	Removed rows G, I,
49	252	95,45	0,043637	0,042110	0,085747	2842,91	9,86	Removed row I
50	264	100,00	0,044323	0,044283	0,088607	3115,45	10,33	Complete
51	251	95,08	0,043660	0,042983	0,086643	2936,77	10,02	Removed random group A
52	238	90,15	0,043127	0,043177	0,086303	2709,88	9,64	Removed random group A, B
53	225	85,23	0,042350	0,041763	0,084113	2510,12	9,25	Removed random group A, B, C
54	238	90,15	0,042947	0,042680	0,085627	2727,17	9,68	Removed random group A, C
55	251	95,08	0,043137	0,043353	0,086490	2919,85	9,97	Removed random group C
56	264	100,00	0,044957	0,044130	0,089087	3119,23	10,20	Complete

Rods of random groups		
A	B	C
G8	K10	A15
J7	H16	A7
K14	K2	H5
D7	F17	M16
O3	G10	D3
C15	P7	N1
D10	B13	Q17
O15	M7	K4
D1	E13	G14
P13	H1	Q9
K17	B4	C17
N11	Q11	B10
B2	Q4	J15